Scientific Research Publishing

American Journal of Molecular Biology, 2022, 12, 11-22
https://www.scirp.org/journal/ajmb
ISSN Online: 2161-6663
ISSN Print: 2161-6620

M_3 Muscarinic Acetylcholine Receptor Antagonist Darifenacin Protects against Pulmonary Fibrosis through ERK/NF-κB/miR-21 Pathway

Ying Liu[1], Yanan Jiang[2], Chao Wang[3], Haiying Zhang[1*], Yan Liu[1*]

[1]Key Laboratory of Tropical Translational Medicine of Ministry of Education, College of Pharmaceutical, Hainan Medical University, Haikou, China
[2]Department of Pharmacology, Harbin Medical University, Harbin, China
[3]Sanya Central Hospital, Sanya, China
Email: *hy0207123@hainmc.edu.cn, *liuyan_gyp@163.com

How to cite this paper: Liu, Y., Jiang, Y.N., Wang, C., Zhang, H.Y. and Liu, Y. (2022) M_3 Muscarinic Acetylcholine Receptor Antagonist Darifenacin Protects against Pulmonary Fibrosis through ERK/NF-κB/miR-21 Pathway. *American Journal of Molecular Biology*, **12**, 11-22.
https://doi.org/10.4236/ajmb.2022.122002

Received: December 13, 2021
Accepted: April 3, 2022
Published: April 6, 2022

Abstract

Idiopathic pulmonary fibrosis is an untreatable lethal lung disease, which is related to the aberrant proliferation of fibroblasts. M_3 muscarinic acetylcholine receptor (M_3-mAChR) activation exerts proliferative effect on various kinds of cells. However, whether M_3-mAChR inhibition has a protective effect on pulmonary fibrosis remains unexplored. A rat model of pulmonary fibrosis was established by intratracheal instillation of bleomycin. Darifenacin was used to block M_3-mAChR. Histological changes were observed using Masson's Trichrome and hematoxylin and eosin (HE) staining. Hydroxyproline was measured by Hydroxyproline detection kit. Transforming growth factor β1 (TGF-β1) and tumor necrosis factor-α (TNF-α) were measured by enzyme-linked immunosorbent assay (ELISA). *In vitro*, pulmonary fibroblasts were isolated from lungs of neonatal rat. After treatment, the cell viability, Hydroxyproline level was measured by MTT and Hydroxyproline detection kit respectively. The expression level of extracellular signal-regulated kinase (ERK), nuclear factor kappa-B (N-NF-κB), and microRNA-21 (miR-21) was detected by western blot or quantitative real-time PCR (qRT-PCR). Darifenacin relieved the fibrotic effects provoked by bleomycin. The expression level of hydroxyproline, TGF-β1 and TNF-α level was all downregulated after darifenacin treatment. In lung fibroblasts, darifenacin decreased cell viability and hydroxyproline level induced by bleomycin. Besides, phosphorylation-ERK and nuclear N-NF-κB protein level was downregulated, as well as miR-21 level. M_3-mAChR antagonist darifenacin attenuates bleomycin-induced pulmonary fibrosis in rats, which may relate to the ERK/NF-κB/miRNA-21

signaling pathway.

Keywords

Pulmonary Fibrosis, M_3 Muscarinic Acetylcholine Receptor, Darifenacin

1. Introduction

Pulmonary fibrosis is a common clinical manifestation of various types of lung diseases, including pneumoconiosis, interstitial pneumonia, idiopathic interstitial pneumonias, etc. Idiopathic pulmonary fibrosis (IPF) is one of the most common and severe pulmonary fibrosis diseases, and the mortality is increasing in recent years [1]. Anti-inflammatory, immunosuppressive and corticosteroid agents were used for the treatment of pulmonary fibrosis in clinical. Unfortunately, the effects of these drugs were still not satisfying. At present, there is no treatment that can cure IPF. Two drugs, pirfenidone and nintedanib can slow disease progression, but neither drug improves or even stabilizes lung function, or improves quality of life, and both therapies have tolerability issues. Thus, finding new strategies for the treatment of pulmonary fibrosis is urgently needed. Additional treatment trials are needed, because current treatments for IPF have limited efficacy.

Recent studies indicate that fibroblast proliferation, activation, differentiation and extracellular matrix uncontrolled accumulation would result in the destruction of alveolar architecture, followed by a loss of lung function [2] [3]. None of the available therapies has a significant effect on airway and lung tissue remodelling in fibrosis. The most important question is "why are pathological changes of the lung structure irreversible and resistant to drugs?" Many drugs have the potential to reduce remodelling mechanisms *in vitro* but fail in clinical trials. New evidence suggests that muscarinic receptor inhibitors have the potential to improve lung function through modifying tissue remodelling. For example, a muscarinic receptor antagonist tiotropium bromide is used for pulmonary in the clinic for its anti-proliferative activity [4] [5]. The other new long-acting muscarinic antagonist can also suppress the differentiation of human fibroblast [6]. However, the role of muscarinic receptors in lung remodelling, needs to be further investigated.

As the main receptor of acetylcholine, muscarinic acetylcholine receptor subtypes M_1, M_2 as well as M_3 are expressed in fibroblasts and myofibroblasts [7]. Collagen secretion and proliferation of human lung fibroblasts are induced by muscarinic receptor stimulation [8] [9] [10] [11] [12]. The M_3 selectivity of the M_3-mAChR antagonist darifenacin is unique among antimuscarinics. This M_3 selectivity could confer advantages in patients who have cardiovascular side effects (tachycardia), impaired cognition, complaints of dizziness, or sleep disturbances. Based on these findings, daphnemycin is effective and well tolerated.

More importantly, it is a drug that minimizes the risk of safety related adverse reactions. However, whether M_3-mAChR antagonist has effect on pulmonary fibrosis remains unelucidated. This study was designed to investigate the effects of darifenacin on pulmonary fibrosis and explore the underlying mechanism.

2. Materials and Methods

2.1. Reagents

Bleomycin was purchased from Nippon Kayaku Co. (Chiyoda-ku, Tokyo, Japan). Anti-GAPDH, anti-H3, Alex a FluorH 800 goat anti-rabbit IgG or anti-mouse IgG were purchased from Santa Cruz Biotechnology (Santa Cruz, CA, USA). Anti-ERK and anti-pERK antibody were bought from Cell Signaling Technology (Boston, USA). Anti-nuclear factor-(NF-) κB p65 were bought from Bioss (Bioss, Beijing, China). TRIzol Reagent was obtained from Invitrogen (Carlsbad, CA, USA). Reverse transcriptase kit was from Promega (Madison, Wisconsin, USA). Hydroxyproline detection kit was obtained from Jiancheng Bioengineering Institute (Nanjing, China). Rat TNF-α and TGF-β1 ELISA kit were purchased from BOSTER (Wuhan, Hunan, China). Methyl thiazolyl tetrazolium (MTT) and darifenacin were from Sigma (St Louis, MO, USA). BCA Protein Assay kit was brought from Pierce (Rockford, IL, USA). The mirVana™ qRT-PCR Detection miRNA Kit was from Ambion (Austin, TX, USA). Primers of miR-21 were from Gene Pharma (Shanghai, China). Dulbecco's modified Eagle's medium (DMEM), fetal bovine serum (FBS) were purchased from Life Technologies, Inc (Carlsbad, CA, USA).

2.2. Animals

Wistar rats (6 - 8 w) weighing 200 - 250 g and neonatal rats (1 - 3 d) were obtained from the experimental animal center of the Second Affiliated hospital of Harbin Medical University. All experimental protocols were pre-approved by the Experimental Animal Ethic Committee of Harbin Medical University, China. Use of animals followed the Guide for the Care and Use of Laboratory Animals published by the US National Institutes of Health (NIH Publication No. 85-23, revised 1996).

2.3. Bleomycin-Induced Pulmonary Fibrosis Rat Model

Briefly, at day 0, rats were anesthetized with intraperitoneal injection of 2% pentobarbital (0.5 ml/100g) and intratracheally instilled bleomycin (5 mg/kg) to establish the model of rat pulmonary fibrosis. And the sham-operated control group rats (n = 7) were instilled saline instead of bleomycin in the same way. Rats of the bleomycin-induced pulmonary fibrosis model were randomly divided into bleomycin group (n = 7) and darifenacin group (n = 7). Darifenacin (5 mg/kg/day) was administered intraperitoneally in darifenacin group. bleomycin group with saline (0.9 percent sodium chloride) in the same manner. Seven days after treatment, the rat blood samples were collected via a tail vein from each group. Three weeks after bleomycin or saline administration, rats in each

group were sacrificed and the lung tissues were harvested for the following experiment.

2.4. Primary Culture of Neonatal Rat Pulmonary Fibroblasts

Pulmonary fibroblasts were isolated from neonatal rats. Briefly, whole lung was isolated and collected as quickly as possible. After washed out the residue blood with PBS, the lung tissues were chopped into suitable small pieces into and rinsed again in PBS. All of operations were performed on ice. Then the tissue fragments were digested with repetitive 0.125% trypsinization and shaken gently for suitable time in 37˚C water-bath. The supernatant was collected in DMEM containing 10% (vol/vol) fetal bovine serum (supernatant/DMEM = 1/1) and then kept at 4˚C provisionally. After filtering, the filtrate was collected and centrifuged for 5 min 1500 round/min. Finally, the cells were resuspended in the new culture medium DMEM, which contained 10% fetal bovine serum and 1% double-antibiotic (penicillin and etiolation). Resuspended cells were then plated in one culture bottle and incubated in a humidified incubator (95% O_2, 5% CO_2, 37˚C) for 1.5 h to remove non-fibroblast contamination.

2.5. Histological Analysis

Masson's Trichrome and hematoxylin and eosin (HE) staining were used to observe the changes of lung histological. The middle lobes of left lung were fixed in 10% buffered paraformaldehyde (pH 7.4) for a week and then embedded in paraffin blocks. The lung lobes fixed were cut longitudinally into 5-μm-thick sections and then stained with Masson's Trichrome and HE via Ashcroft scoring method, respectively.

2.6. Hydroxyproline Assay

Hydroxyproline level of lung tissues (40 - 60 mg per lung) or cell-culture medium of pulmonary fibroblasts was determined by hydroxyproline detection kit following the manufacturer's direction and described using micrograms of hydroxyproline per gram of wet weight (mg/g).

2.7. Enzyme-Linked Immunosorbent Assay (ELISA)

ELISA for the measurement of cytokine TNF-α and TGF-β1 level in serum and cell culture supernatants were performed according to the manufacturer's instructions.

2.8. MTT Assay

Pulmonary fibroblasts (2×10^4 cells/well) were seeded in 96-well plates with 200 μl of medium per well. After 24 h, the cells were treated with darifenacin. After incubation, 10 μl of MTT reagents (5 mg/ml) was added and incubated for 4 h under the same conditions. Then, the medium was removed from the plate, and the formazan was dissolved with 150 μl DMSO. The absorbance (OD) at 490 nm was measured by a microplate reader.

2.9. Western Blot Analysis

Total and nuclear proteins were extracted from lung tissues and primary culture pulmonary fibroblasts. The content of protein was then measured by BCA protein assay kit. The equal amounts of proteins samples were separated by 10% SDS-PAGE and transferred to nitrocellulose membranes. The membranes were blocked with 5% nonfat milk for 2 h at room temperature and then incubated with corresponding antibodies at 4˚C over-night. After that, the nitrocellulose membrane was washed 3 times with PBS containing 0.05% Tween-20 (PBS-T) followed by incubated with secondary antibodies (1:10,000) for 1h at room temperature. The images were captured on the Odyssey Infrared Imaging System (LI-COR Bioscience, Lincoln, NE, USA) and band intensity (area × optical density) was quantified using Odyssey v1.2 software. GAPDH was served as an internal control.

2.10. RNA Isolation and Quantitative RT-PCR

Total RNA was extracted using TRIzol Reagent. First-strand complementary DNA (cDNA) was synthetized using a reverse transcriptase kit according to the manufacturer's instructions. Those cDNA were used as the template for quantitative RT-PCR (qRT-PCR) analysis on an ABI 7500 fast Real Time system (Applied Biosystems, Foster City, CA, USA), with U6 as an internal control. The sequences of the primers were as follows: U6,
5'-CTCCGATAGATCTGCCCTCTTGAA-3' (forward),
5'-CGCTTCACGAATTTGCGTGTCAT-3' (reverse); miR-21,
5'-GGGGTAGCTTATCAGACTGATG-3' (forward),
5'-TGTCGTGGAGCGGCAATTG-3' (reverse); collagen I,
5'-GCTCCTCTTAGGGGCCACT-3' (forward),
5'-CCACGTCTCACCATTGGGG-3' (reverse);
α-SMA,5'-AGGGAGTAATGGTTGGAATGG-3' (forward),
5'-GGTGATGATGCCGTGTTCTA-3' (reverse); GAPDH,
5'-TGTGGGCATCAATGGATTTGG-3' (forward),
5'-ACACCATGTATTCCGGGTCAAT-3' (reverse).

2.11. Statistical Analysis

Average data were expressed as mean ± standard error of the mean (SEM). Comparisons among multiple groups were analyzed by one-way analysis of variance (one-way ANOVA) followed by Bonferroni-corrected post-hoc tests were carried out using SPSS 13.0. A two-tailed P value < 0.05 indicated a statistically significant difference.

3. Results

3.1. Darifenacin Improves the Histological Changes of Bleomycin-Induced Pulmonary Fibrosis in Rats

The changes of lung histological were observed by HE staining and Masson's

Trichrome staining. The signs of inflammatory cell infiltration and fibrotic changes were notable in the bleomycin group. Meanwhile, the alveolar septa became significant thickened compared with the control group in HE staining (Figure 1(a) and Figure 1(c)). Moreover, alveolar spaces became smaller even dent, accompanied by deposition of extensive blue collagen in Masson's Trichrome staining (Figure 1(b) and Figure 1(d)). However, in the darifenacin group, the inflammatory infiltration, fibrotic and alveolar septa changed, as well as deposition of blue collagen all were remarkably alleviated compared with the bleomycin group.

3.2. Effect of Darifenacin on Bleomycin Induced Pulmonary Fibrosis

The hydroxyproline levels in lung tissues among three groups were assessed using hydroxyproline detection kit (Figure 2(a)). In bleomycin group, the hydroxyproline level was significantly increased compared with the sham-operated control group. However, the increase of hydroxyproline induced by bleomycin was attenuated by administration with darifenacin. The expression level of cytokine

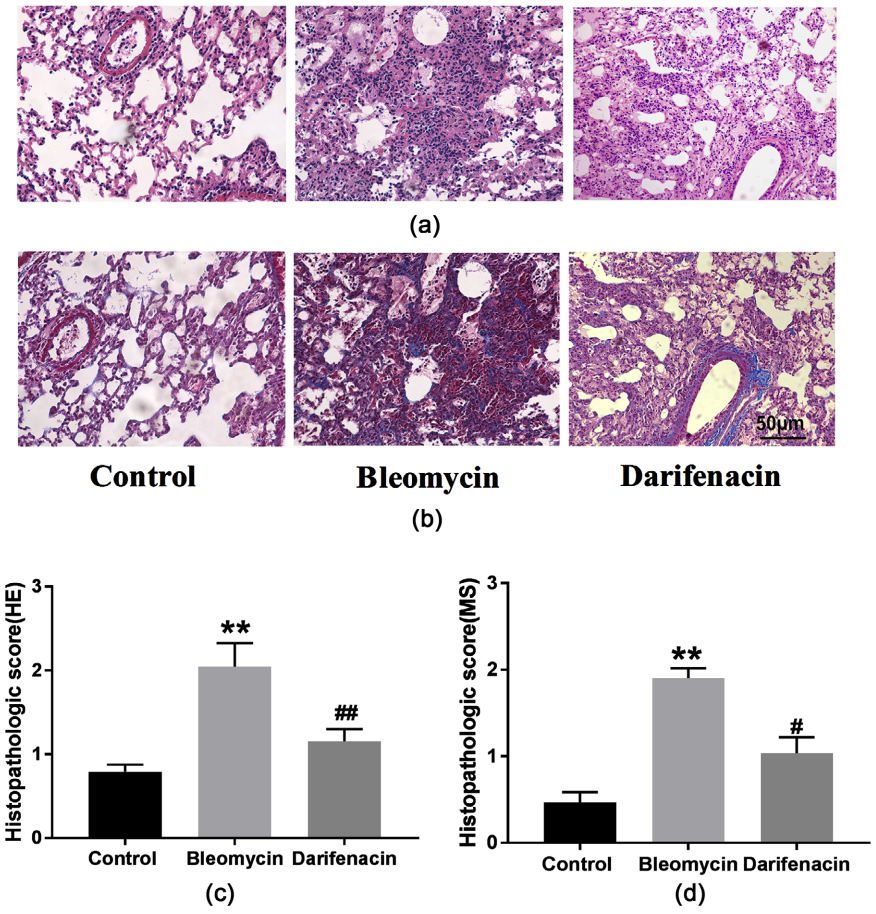

Figure 1. The pulmonary pathological changes. ((a), (c)) hematoxylin and eosin (HE) staining; ((b), (d)) Masson's Trichrome staining. $^{**}P < 0.01$ versus control group, $^{\#\#}P < 0.01$ versus bleomycin group; n = 3.

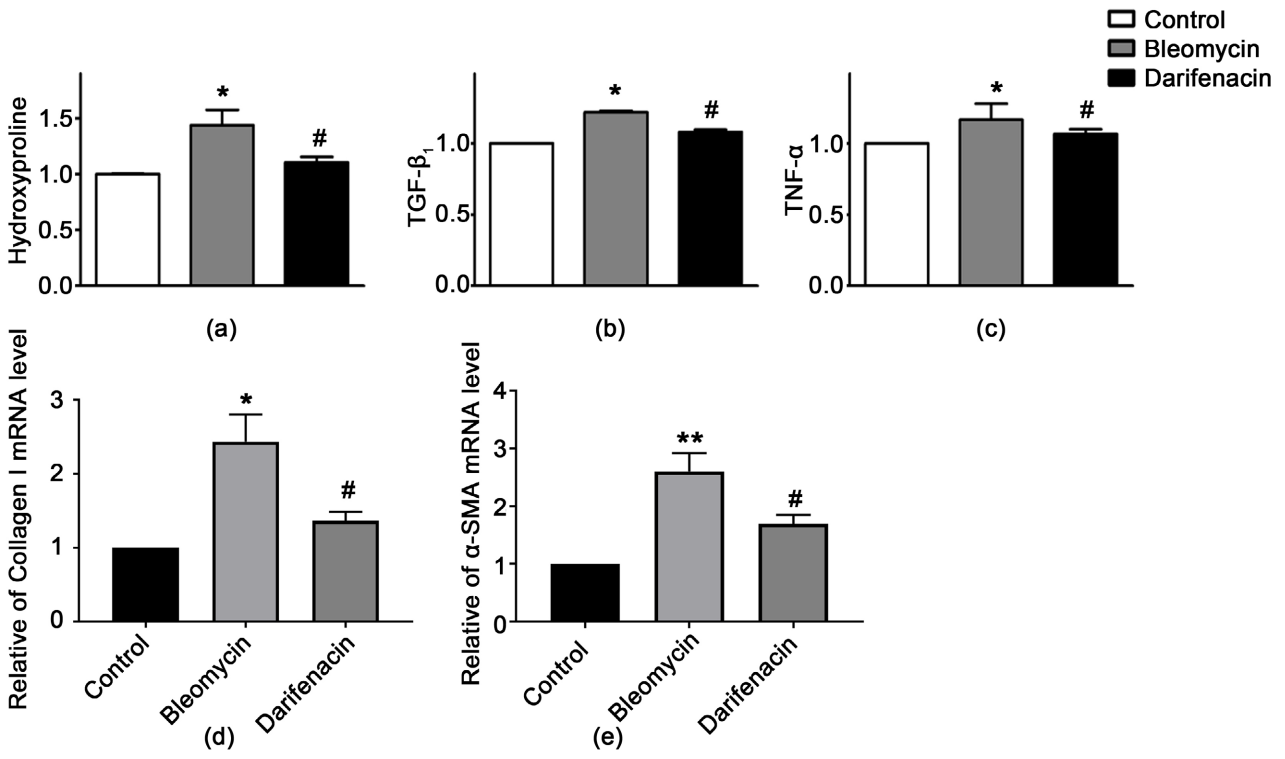

Figure 2. Effect of darifenacin on bleomycin induced pulmonary fibrosis. (a) Darifenacin inhibited bleomycin induced increase of hydroxyproline level in lung tissues. ((b), (c)) Darifenacin inhibited bleomycin induced increase of TGF-β1 and TNF-α level in serum. ((d), (e)) Real-time PCR results showing that darifenacin decreases the fibroblast marker genes, collagen I and α-SMA in MRC-5 cells. $^{*}P < 0.05$, $^{**}P < 0.01$ versus control group, $^{\#}P < 0.05$ versus bleomycin group; n = 3.

TGF-β1 and TNF-α in serum were assessed by ELISA. The levels of cytokines in the two groups were notable higher than control group (**Figure 2(b)** and **Figure 2(c)**). As we expected, after darifenacin treatment, all the cytokines level was decreased noticeably compared with bleomycin group.

Then, we examined the therapeutic effect of the darifenacin in the bleomycin-induced fibrotic process in human pulmonary fibroblasts (MRC-5 cells) by qPCR. Administration of darifenacin significantly decreased the expression of collagen I and α-SMA in bleomycin-treated MRC-5 cells (**Figure 2(d)** and **Figure 2(e)**).

3.3. Darifenacin Inhibited the Proliferation of Rat Pulmonary Fibroblasts

Pulmonary fibroblasts derived from neonatal rats were used for proliferation assay. Pulmonary fibroblasts derived from neonatal rats were used for proliferation assay. Using MTT assay to measure the viability of pulmonary fibroblasts and nintedanib as a positive control, the results shown that cell viability of darifenacin and nintedanib groups decreased significantly compared with the control group (**Figure 3(a)**). The proliferation of cells was reduced to 53% by 1 μM darifenacin and that to 70% by 1 μM nintedanib, respectively. Besides, both darifenacin and nintedanib caused a significant decrease of the Hydroxyproline

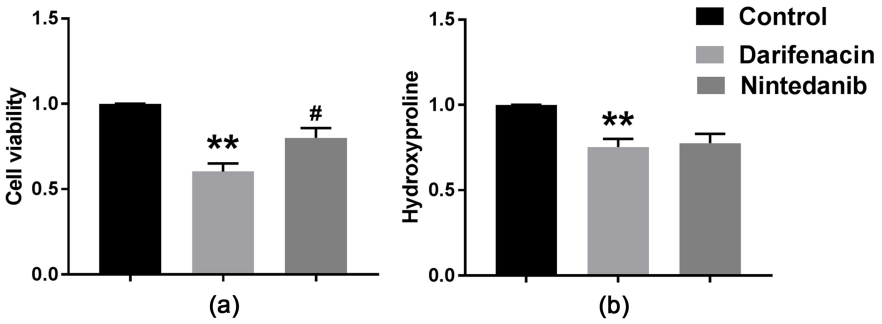

Figure 3. Effect of darifenacin on cell viability and hydroxyproline level in cultured rat pulmonary fibroblasts. (a) Darifenacin reduced the cell viability of pulmonary fibroblasts. (b) Darifenacin reduced hydroxyproline level in pulmonary fibroblasts. $^{**}P < 0.01$, $^{*}P < 0.05$ versus control group; $^{\#}P < 0.05$ versus darifenacin group, n = 4.

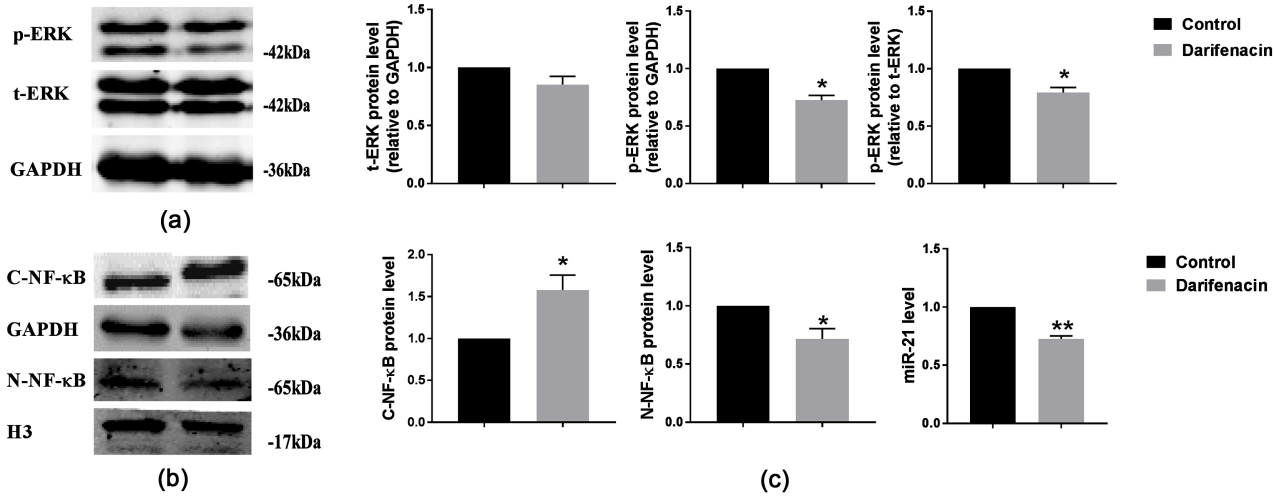

Figure 4. Effect of darifenacin on ERK and NF-κB protein expression and miR-21 level in cultured rat pulmonary fibroblasts. (a) Darifenacin inhibited phospho-ERK (P-ERK) expression. (b) Darifenacin inhibited nuclear-NF-κB (N-NF-κB) expression. (c) Darifenacin inhibited miR-21 expression. GAPDH as an internal control normalized ERK or C-NF-κB band and H3 as an internal control normalized N-NF-κB band for western blot. U6 as an internal control to normalize miR-21 expression. Phospho-protein level was relative to total protein level. $^{*}P < 0.05$ versus control group, $^{**}P < 0.01$ versus control group; n = 3.

level in pulmonary fibroblasts (Figure 3(b)). In the present study, both nintedanib and pirfenidone inhibited the proliferation of fibroblastic cells. At the same concentration, the effect of darifenacin was better than nintedanib.

3.4. Darifenacin Inhibited the Expression Level of ERK, NF-κB and miR-21 in Rat Pulmonary Fibroblasts

To investigate whether ERK, NF-κB and miR-21 were involved in the antifibrotic effect of darifenacin on pulmonary fibrosis, we identified the ERK activation, NF-κB nuclear translocation, and miR-21 expression in pulmonary fibroblasts. The total protein level of ERK (t-ERK) remained unchanged between the two groups. However, the protein expression of p-ERK was markedly decreased in darifenacin group (Figure 4(a)). Additionally, further data showed that administration of darifenacin to pulmonary fibroblasts markedly reduced the nuclear

NF-κB (N-NF-κB) and enhanced the cytoplasmic NF-κB (C-NF-κB) expression (**Figure 4(b)**). Besides miR-21 level was also decreased in darifenacin group (**Figure 4(c)**).

4. Discussion

Pulmonary fibrosis is a progressive and lethal interstitial lung disease characterized by deposit collagen and fibroblastic foci containing fibroblasts/myofibroblasts [13]. Though substantial progress has been made in the pathophysiology study of pulmonary fibrosis over the past decades, the pathogenesis of pulmonary fibrosis was still not fully elucidated. Thus, searching for new and effective therapeutic approaches is vitally important. Chemokines, growth factors and profibrotic cytokines are all taken part in the sophisticated progression. Among these cytokines, TGF-β1 and TNF-α perform important roles in the pathogenesis of pulmonary fibrosis. Many researchers have indicated that TGF-β1, as one of TGF-β three isoforms, promotes proliferation and differentiation of lung fibroblasts, increases secretion of collagen in lung fibrosis [14]. Moreover, it is generally recognized that TGF-β1 cascade initiates with type I and type III ligand binding, subsequently activated Smad signaling to promote lung fibroblasts [15]. Evidences showed that level of TNF-α was elevated in serum samples of pulmonary fibrosis [15]. Moreover, in the pulmonary interstitium, TNF-α overexpression, like TGF-β1, also leads to abnormal accumulation of fibroblast and extracellular matrix, and soluble TNF-α mediates the transition from inflammation to fibrosis [16].

In the present study, we found that M_3-mAChR antagonist darifenacin attenuated bleomycin-induced pulmonary fibrosis in rat. And there is no relevant clinical evidence that darifenacin has side effects on other organs, but we will further explore its side effects in future research. The histological alterations of fibrosis were reduced with darifenacin treatment. Besides serum TGF-β1 and TNF-α expression were also downregulated. We then conducted the experiment *in vitro* using primary cultured rat pulmonary fibroblasts. After incubated with darifenacin, cell viability and hydroxyproline level were significantly downregulated compared with that in control group. Growing studies demonstrated that ERK was involved in the processes of pulmonary fibrosis [17]. Our results found that p-ERK protein level was downregulated in rat pulmonary fibroblasts treated with darifenacin. It has been reported that ERK activation could upregulate nuclear NF-κB expression [18]. The blockade of NF-κB related signaling pathways could attenuate pulmonary fibrosis [19]. Our experiment found that darifenacin could downregulate nuclear NF-κB protein level in rat pulmonary fibroblasts.

As a nuclear transcription factor, NF-κB could regulate the transcription of various genes. MicroRNA (miRNA) was a kind of noncoding RNA, which is also involved in the process of pulmonary fibrosis. Numerous microRNAs were markedly changed during pulmonary fibrosis. Thereinto, microRNA-21 (miR-21) was significantly up-regulated in the lung of bleomycin-instilled mice and pos-

sesses therapeutic potential [20]. Besides, NF-κB directly upregulated the expression of miR-21 [21]. To confirm these findings, our experiment observed the downregulation of miR-21 and NF-κB. It is further demonstrated that darifenacin may regulate miR-21 and NF-κB pathway to treat pulmonary fibrosis.

To our knowledge, this is the first report demonstrated that M_3-mAChR antagonist may have therapeutic potential in the prevention or treatment of pulmonary fibrosis, and verified the potential underlying mechanisms. In summary, we found that darifenacin attenuated BLM-induced fibrosis in a rat model and pulmonary fibroblasts. These findings indicate that the major mechanism responsible for the effects of darifenacin involves inhibition of the ERK, NF-κB and miR-21 signaling pathway. Based on these results, we suggest that darifenacin may be considered a potential treatment for IPF. Future studies should determine the optimal dosage of darifenacin and identify other mechanisms that contribute to anti-pulmonary fibrosis.

Funding

This work was supported by the Natural Science Foundation of Hainan Province (No.2019RC225) and the National Natural Science Foundation of China (No. 81960676).

Conflicts of Interest

The authors declare that they have no conflict of interest.

References

[1] Marshall, D.C., Salciccioli, J.D., Shea, B.S. and Akuthota, P. (2018) Trends in Mortality from Idiopathic Pulmonary Fibrosis in the European Union: An Observational Study of the WHO Mortality Database from 2001-2013. *The European Respiratory Journal*, **51**, Article ID: 1701603. https://doi.org/10.1183/13993003.01603-2017

[2] Ahrman, E., Hallgren, O., Malmstrom, L., Hedstrom, U., Malmstrom, A., Bjermer, L., Zhou, X.H., Westergren-Thorsson, G. and Malmstrom, J. (2018) Quantitative Proteomic Characterization of the Lung Extracellular Matrix in Chronic Obstructive Pulmonary Disease and Idiopathic Pulmonary Fibrosis. *Journal of Proteomics*, **189**, 3-33. https://doi.org/10.1016/j.jprot.2018.02.027

[3] Munguia-Reyes, A., Balderas-Martinez, Y.I., Becerril, C., Checa, M., Ramirez, R., Ortiz, B., Melendez-Zajgla, J., Pardo, A. and Selman, M. (2018) R-Spondin-2 Is Upregulated in Idiopathic Pulmonary Fibrosis and Affects Fibroblast Behavior. *American Journal of Respiratory Cell and Molecular Biology*, **59**, 65-76. https://doi.org/10.1165/rcmb.2017-0115OC

[4] Gregory, J.A., Kemi, C., Ji, J., Karen, J., Delin, I., Gerde, P., Pieper, M.P., Adner, M. and Larsson, K. (2018) Effects of Tiotropium Bromide on Airway Hyperresponsiveness and Inflammation in Mice Exposed to Organic Dust. *Pulmonary Pharmacology & Therapeutics*, **48**, 203-210. https://doi.org/10.1016/j.pupt.2017.12.004

[5] Ohbayashi, H. (2017) Comparison of the Rapid Effects of Single Inhalations of Formoterol and Tiotropium Bromide on Respiratory Function and COPD Symptoms in a Randomized Crossover Study. *Respiratory Investigation*, **55**, 348-356. https://doi.org/10.1016/j.resinv.2017.07.004

[6] Milara, J., Serrano, A., Peiro, T., Gavalda, A., Miralpeix, M., Morcillo, E.J. and Cortijo, J. (2012) Aclidinium Inhibits Human Lung Fibroblast to Myofibroblast Transition. *Thorax*, **67**, 229-237. https://doi.org/10.1136/thoraxjnl-2011-200376

[7] Pieper, M.P., Chaudhary, N.I. and Park, J.E. (2007) Acetylcholine-Induced Proliferation of Fibroblasts and Myofibroblasts *in Vitro* Is Inhibited by Tiotropium Bromide. *Life Sciences*, **80**, 2270-2273. https://doi.org/10.1016/j.lfs.2007.02.034

[8] Matthiesen, S., Bahulayan, A., Kempkens, S., Haag, S., Fuhrmann, M., Stichnote, C., Juergens, U.R. and Racke, K. (2006) Muscarinic Receptors Mediate Stimulation of Human Lung Fibroblast Proliferation. *American Journal of Respiratory Cell and Molecular Biology*, **35**, 621-627. https://doi.org/10.1165/rcmb.2005-0343RC

[9] Haag, S., Matthiesen, S., Juergens, U.R. and Racke, K. (2006) Muscarinic Receptors Mediate Stimulation of Collagen Synthesis in Human Lung Fibroblasts. *The European Respiratory Journal*, **32**, 555-562. https://doi.org/10.1183/09031936.00129307

[10] Braga, L.E., Granja, M.G., da Silva, G.M., Giestal-de-Araujo, E. and dos Santos, A.A. (2013) PMA Increases M3 Muscarinic Receptor Levels and Decreases Retinal Cells Proliferation through a Change in the Levels of Cell-Cycle Regulatory Proteins. *Neuroscience Letters*, **550**, 29-34. https://doi.org/10.1016/j.neulet.2013.06.045

[11] Xu, R., Shang, C., Zhao, J., Han, Y., Liu, J., Chen, K. and Shi, W. (2015) Activation of M3 Muscarinic Receptor by Acetylcholine Promotes Non-Small Cell Lung Cancer Cell Proliferation and Invasion via EGFR/PI3K/AKT Pathway. *Tumour Biology*, **36**, 4091-4100. https://doi.org/10.1007/s13277-014-2911-z

[12] Yu, H., Xia, H., Tang, Q., Xu, H., Wei, G., Chen, Y., Dai, X., Gong, Q. and Bi, F. (2017) Acetylcholine Acts through M3 Muscarinic Receptor to Activate the EGFR Signaling and Promotes Gastric Cancer Cell Proliferation. *Scientific Reports*, **7**, Article No. 40802. https://doi.org/10.1038/srep40802

[13] Zhao, H., Dennery, P.A. and Yao, H. (2018) Metabolic Reprogramming in the Pathogenesis of Chronic Lung Diseases, Including BPD, COPD, and Pulmonary Fibrosis. *American Journal of Physiology. Lung Cellular and Molecular Physiology*, **314**, L544-L554. https://doi.org/10.1152/ajplung.00521.2017

[14] Shima, H., Sasaki, K., Suzuki, T., Mukawa, C., Obara, T., Oba, Y., Matsuo, A., Kobayashi, T., Mishima, E., Watanabe, S., Akiyama, Y., Kikuchi, K., Matsuhashi, T., Oikawa, Y., Nanto, F., Akiyama, Y., Ho, H.J., Suzuki, C., Saigusa, D., Masamune, A., Tomioka, Y., Masaki, T., Ito, S., Hayashi, K.I. and Abe, T. (2017) A Novel Indole Compound MA-35 Attenuates Renal Fibrosis by Inhibiting both TNF-Alpha and TGF-beta1 Pathways. *Scientific Reports*, **7**, Article No. 1884. https://doi.org/10.1038/s41598-017-01702-7

[15] Huang, C., Wu, X., Wang, S., Wang, W., Guo, F., Chen, Y., Pan, B., Zhang, M. and Fan, X. (2018) Combination of *Salvia miltiorrhiza* and Ligustrazine Attenuates Bleomycin-Induced Pulmonary Fibrosis in Rats via Modulating TNF-Alpha and TGF-Beta. *Chinese Medicine*, **13**, 36. https://doi.org/10.1186/s13020-018-0194-9

[16] Oikonomou, N., Harokopos, V., Zalevsky, J., Valavanis, C., Kotanidou, A., Szymkowski, D.E., Kollias, G. and Aidinis, V. (2006) Soluble TNF Mediates the Transition from Pulmonary Inflammation to Fibrosis. *PLoS ONE*, **1**, e108. https://doi.org/10.1371/journal.pone.0000108

[17] Dong, H., Luo, L., Zou, M., Huang, C., Wan, X., Hu, Y., Le, Y., Zhao, H., Li, W., Zou, F. and Cai, S. (2017) Blockade of Extracellular Heat Shock Protein 90alpha by 1G6-D7 Attenuates Pulmonary Fibrosis through Inhibiting ERK Signaling. *American Journal of Physiology. Lung Cellular and Molecular Physiology*, **313**, L1006-L1015. https://doi.org/10.1152/ajplung.00489.2016

[18] Zeng, A., Yin, J., Li, Y., Li, R., Wang, Z., Zhou, X., Jin, X., Shen, F., Yan, W. and You, Y. (2018) miR-129-5p Targets Wnt5a to Block PKC/ERK/NF-kappaB and JNK Pathways in Glioblastoma. *Cell Death & Disease*, **9**, 394. https://doi.org/10.1038/s41419-018-0343-1

[19] Li, X.H., Xiao, T., Yang, J.H., Qin, Y., Gao, J.J., Liu, H.J. and Zhou, H.G. (2018) Parthenolide Attenuated Bleomycin-Induced Pulmonary Fibrosis via the NF-kappaB/Snail Signaling Pathway. *Respiratory Research*, **19**, 111. https://doi.org/10.1186/s12931-018-0806-z

[20] Sun, N.N., Yu, C.H., Pan, M.X., Zhang, Y., Zheng, B.J., Yang, Q.J., Zheng, Z.M. and Meng, Y. (2017) Mir-21 Mediates the Inhibitory Effect of Ang (1-7) on AngII-Induced NLRP3 Inflammasome Activation by Targeting Spry1 in Lung Fibroblasts. *Scientific Reports*, **7**, Article No. 14369. https://doi.org/10.1038/s41598-017-13305-3

[21] Ni, S.J., Zhao, L.Q., Wang, X.F., Wu, Z.H., Hua, R.X., Wan, C.H., Zhang, J.Y., Zhang, X.W., Huang, M.Z., Gan, L., Sun, H.L., Dimri, G.P. and Guo, W.J. (2018) CBX7 Regulates Stem Cell-Like Properties of Gastric Cancer Cells via p16 and AKT-NF-kappaB-miR-21 Pathways. *Journal of Hematology & Oncology*, **11**, 17. https://doi.org/10.1186/s13045-018-0562-z